Supporting Information for

"New observations negate previous interpretations of surface rupture along the Himalayan Frontal Thrust during the great 1934 Bihar-Nepal earthquake"

Steven G. Wesnousky[1 *], Yasuhiro Kumahara2[1,] Takashi Nakata[2], Deepak Chamlagain[1,3], and Prajwal C. Neupane[3]

[1] Center for Neotectonic Studies and Seismological Laboaratory, University of Nevada, Reno 89557, USA, [2] Graduate School of Education, Hiroshima University, 1-1-1, Kagamiama, Higashi- Hiroshima, Hiroshima 739-8524, Japan, [3] Department of Geology, Tri-Chandra Multiple Campus, Kathmandu, Nepal

Contents of this file

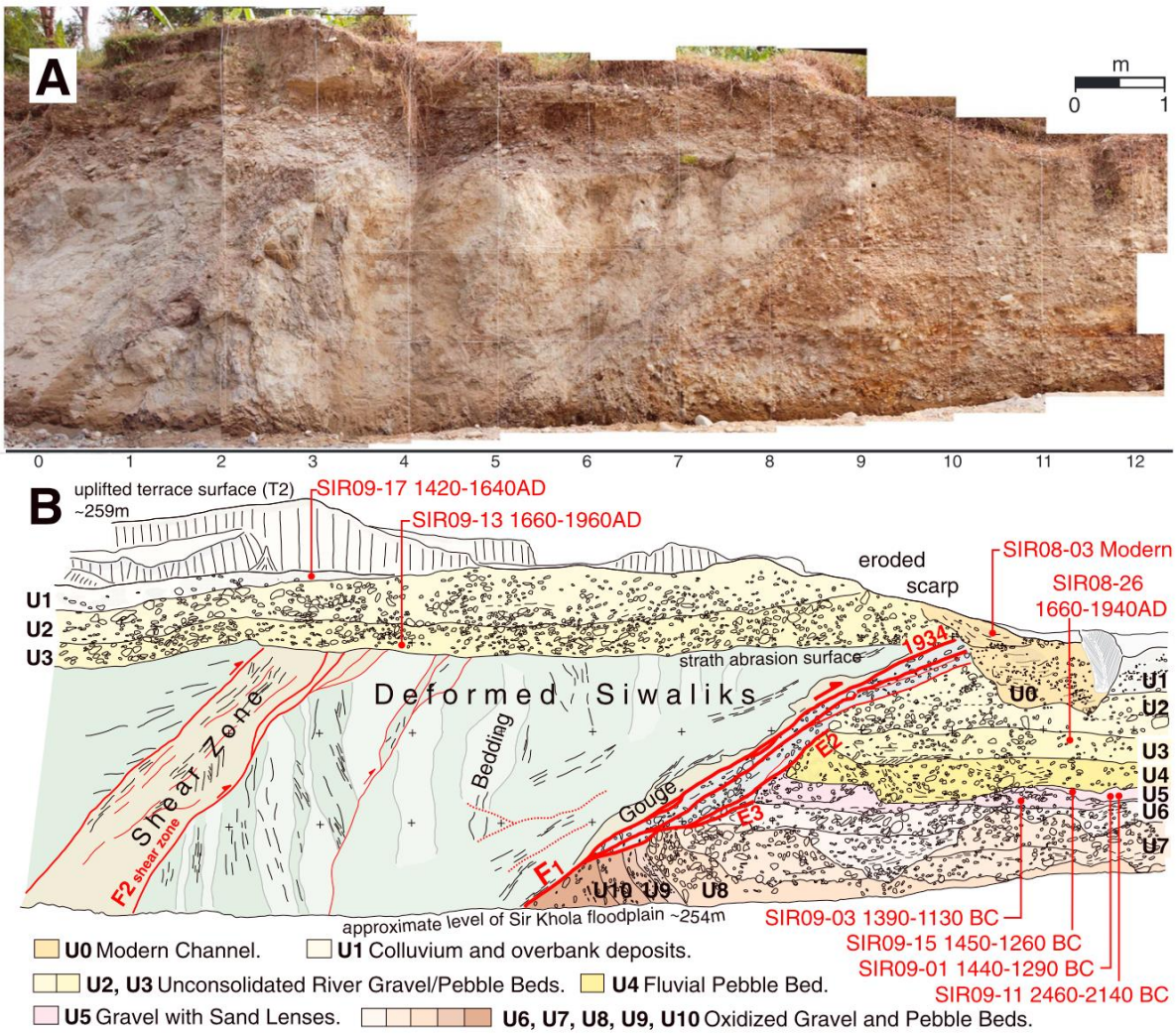

Figure S1. Photo and log of natural exposure at Sir Khola published in Bollinger et al. (2014). Log reflects interpretation that fluvial gravel units U2 and U3 are offset along the shear zone F1, in contrast to the observations presented in this paper and summarized in Figures 4 and 5 of the main manuscript.

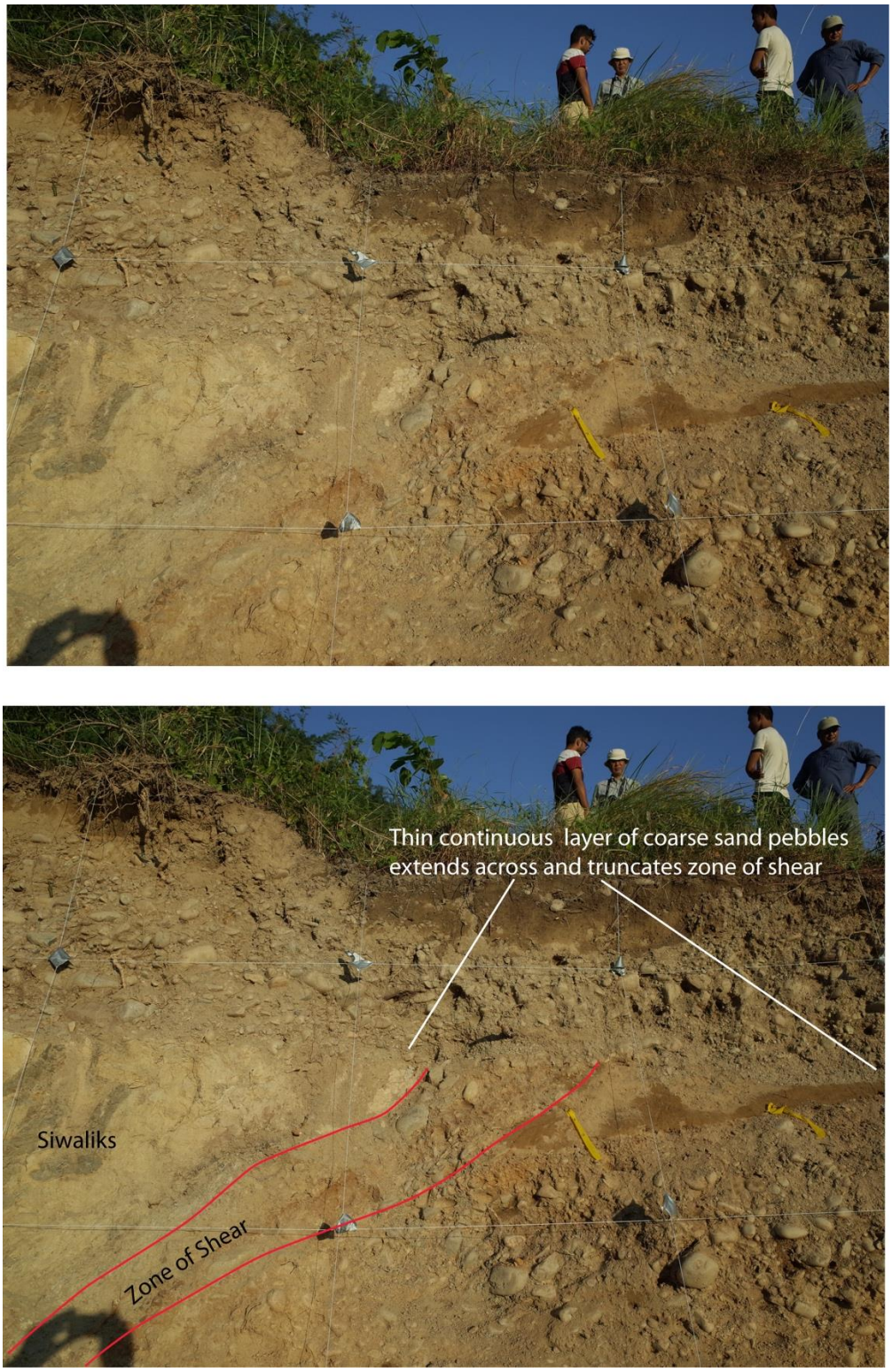

Figure S2a. Images illustrating capping of shear zone by coarse fluvial gravel and distinct coarse sand layer at the basal contact of fluvial gravel. Enlargement of area encompassed by central grid is shown in Figure S2b.

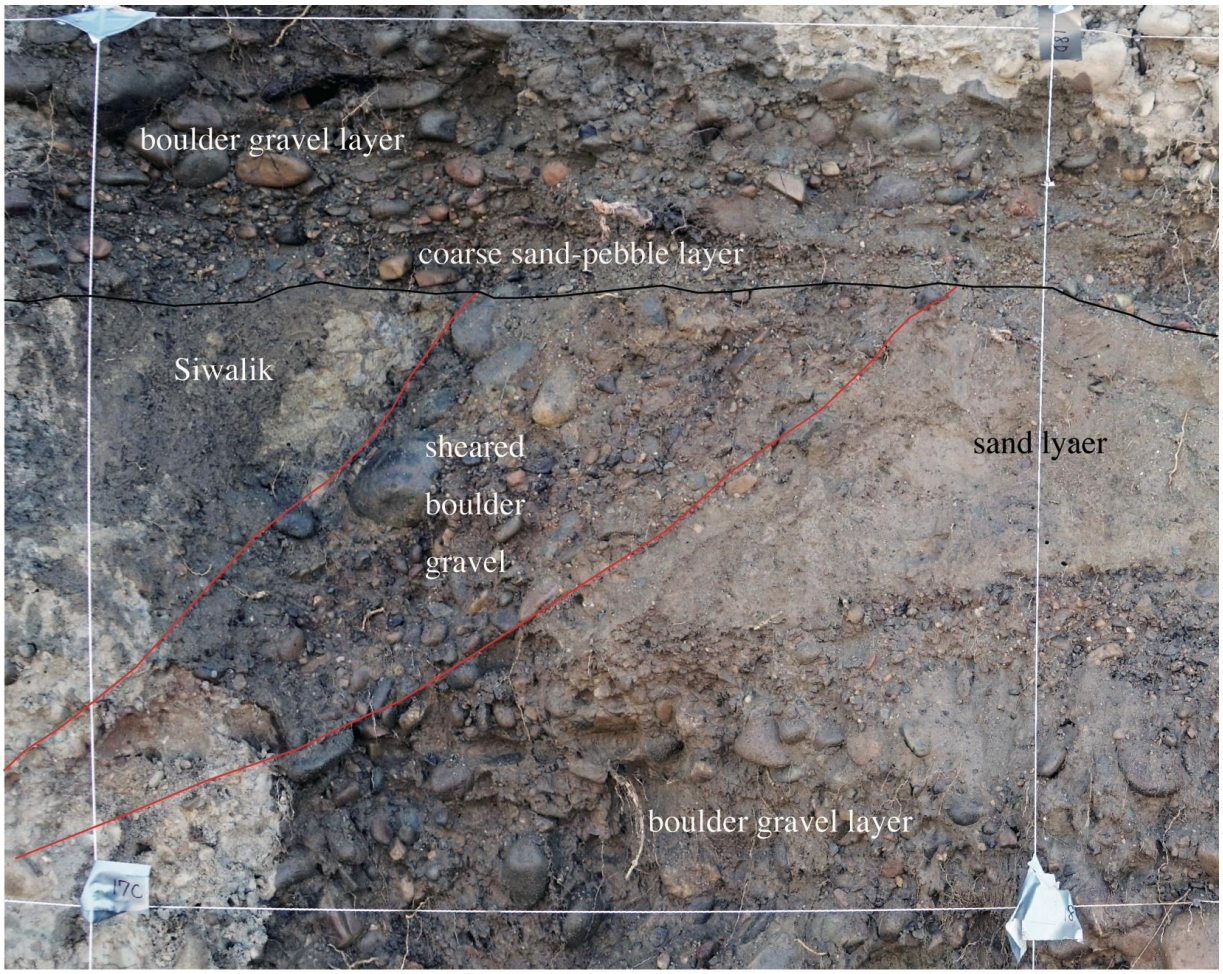

Figure S2b. Enlargement of central grid shown in Figure S2a further illustrates capping of shear. The outcrop was washed with water in effort to enhance the textural characteristics. The regions in upper-right and lower-left of image exhibit high albedo because they were not subject to the water.

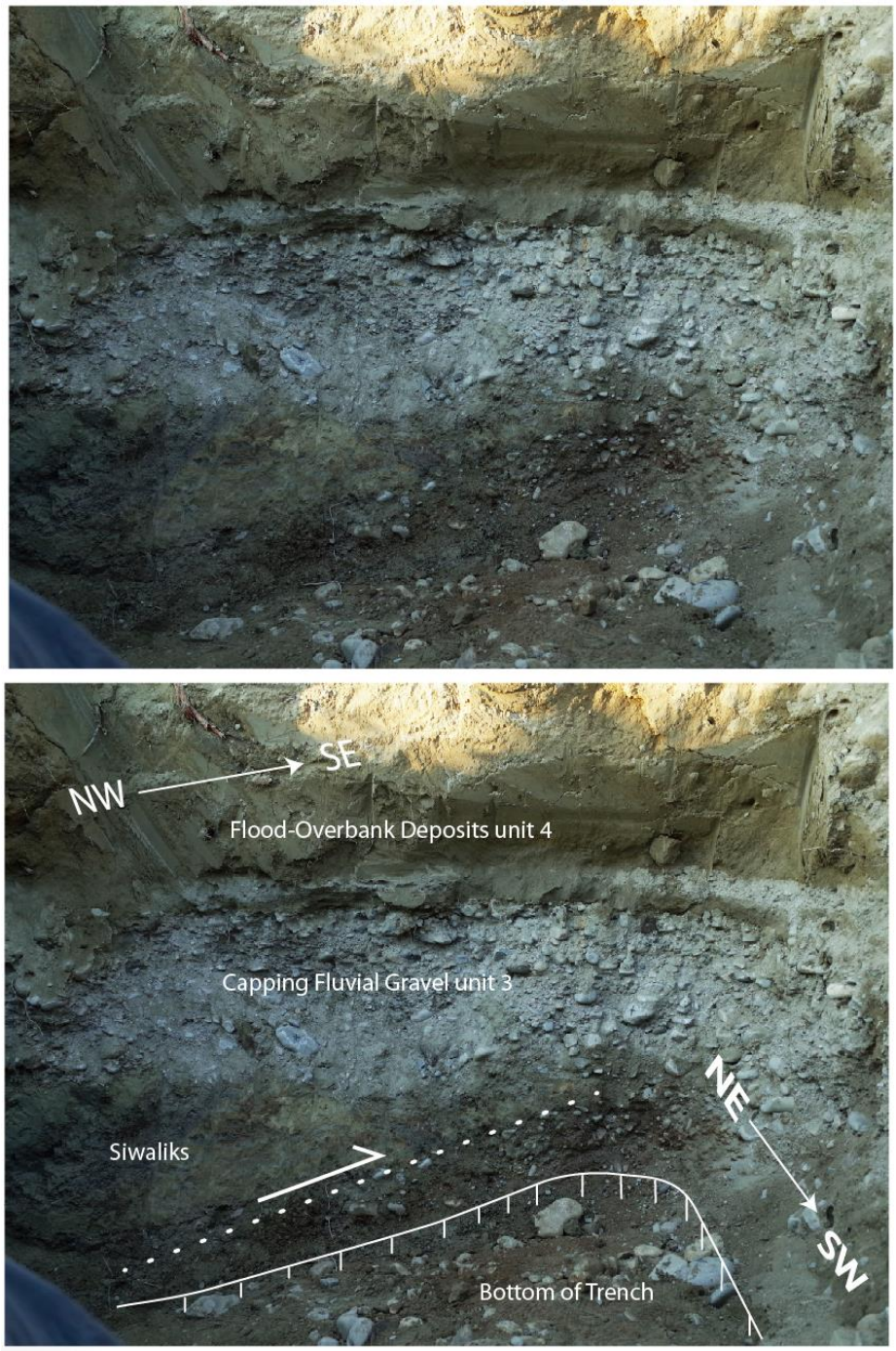

Figure S2c. An additional image of the auxiliary trench exposure showing fluvial gravel layer capping of the shear that has uplifted the Siwlaliks. NW-SE exposure about 1.5-2m length.

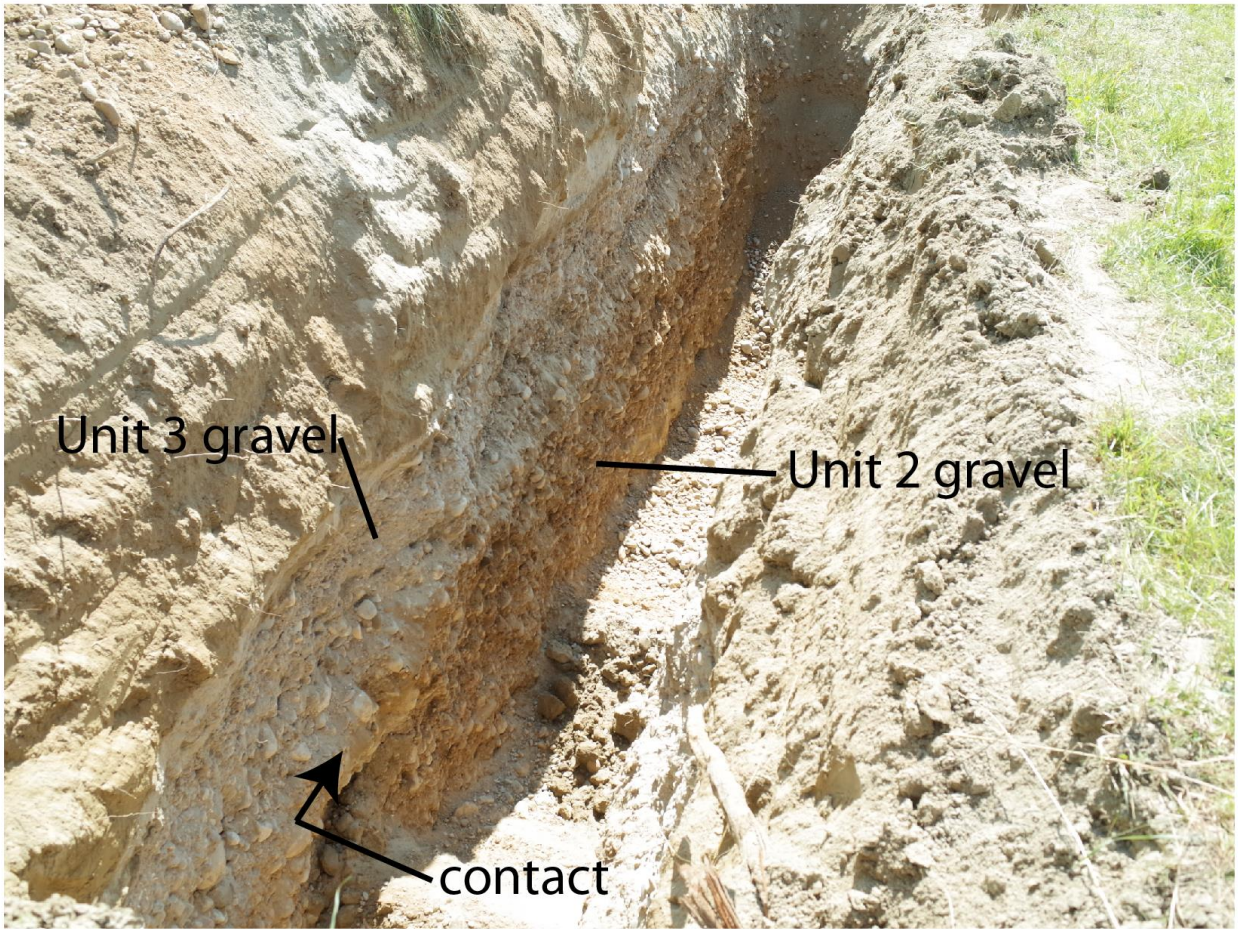

Figure S2d. View of auxiliary trench from perspective of standing above exposure shown in Figure S2c and looking southwest. White fluvial gravels of unit 3 are continuous and unbroken contact with underlying reddish oxidized gravel of unit 2. Length of exposure is about 6 meters. Location and extent of exposure illustrated in Figure 1.

Figure S3. Pole photos illustrate lack of folding and fault scarp in young sediment above the southernmost trace of the HFT observed in the natural exposure that is sketched in Figures 4 and 5 of the main text.

UNIVERSITY OF ARIZONA AMS LABORATORY

Wesnousky, S. (AA110798 - AA110803) – Radiocarbon Analytical Report

Summary Page

The following analytical report contains 14C analysis from the University of Arizona. This report contains:

1. Summary page, includes data qualifiers, non-conformances, and data summary (page 1)
2. Individual sample reports (pages 2-7)

Data Qualifiers: Fraction Modern Carbon and Radiocarbon Age were calculated as weighted averages of combined machine runs to reduce overall error. A small sample correction is applied to samples with a carbon mass less than 0.50 mg.

Non-Conformances: One sample (AA110800) was not measured because it was too small. This sample was observed to be mostly sand and quartz.

Report Generation Date: 1/30/2018

Date: 1/30/2018

Data Summary

AA	lab #	sample ID	MATERIAL	MASS (mg)	d13C value	Fraction Modern	14C age BP
AA110798	X32493	S1	charcoal	1.79	-23.8	0.9852 +- 0.0022	120 +- 18
AA110799	X32494	S2	charcoal	1.19	-25.6	0.9848 +- 0.0022	123 +- 18
AA110800	X32495	S3	charcoal	x	x	Sample too	small
AA110801	X32496	S4	charcoal	0.64	-26.0	0.8302 +- 0.0020	1495 +- 19

Figure S4a. Summary page of analytical report for 14C ages from University of Arizona AMS lab for samples S1, 2, 3, and 4. The counting uncertainties for these ages are much less than for dates reported in Sapkota et al. (2013) and Bollinger et al. (2014). The corrected calendar ages for S1, S2, and S4 shown in Figure 4b are determined with Oxcal v4. 3.2. (https://c14.arch.ox.ac.uk/oxcal/OxCal.html) with the IntCal13 atmospheric curve of Reimer et al. (2013).

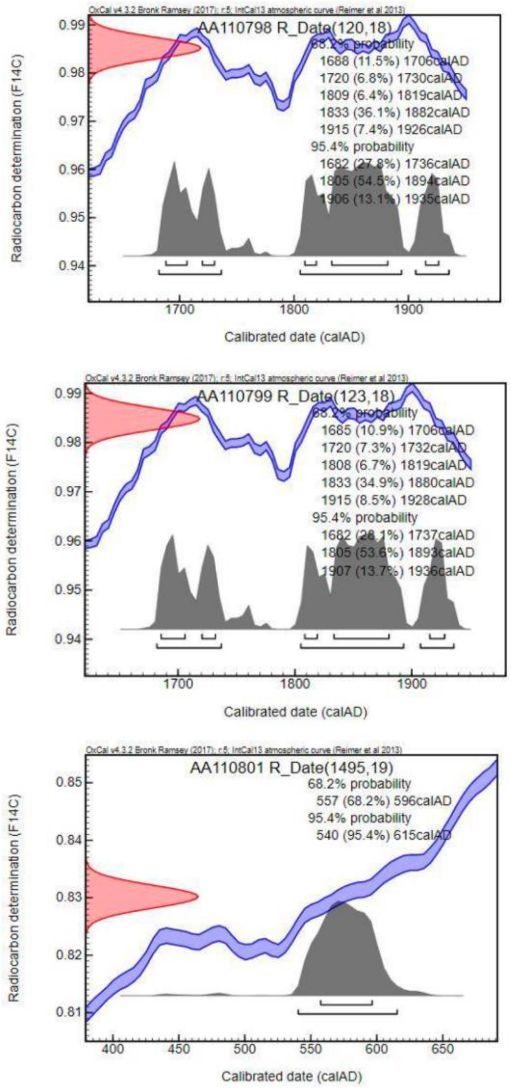

Figure S4b. Dendrochronologically corrected probability distribution of age of samples S1 (upper), S2 (middle) and S4 (lower) calculated with Oxcal v4.3.2. (https://c14.arch.ox.ac.uk/oxcal/OxCal.html) with the IntCal13 atmospheric curve of Reimer et al. (2013). The dendrochronologically corrected ages of S1, S2, and S3 are to 95% confidence limits 1632-1935AD, 1682-1936AD, and 557-615 AD, respectively. The individual runs of S1 and S2 with OxCal illustrate that statistically the ages of the samples S1 and S2 most likely predate 1934. The same is true for those reported by Sapkota et al. (2013) and Bollinger et al. (2014) for their samples taken from the same deposits as S1 and S2.

A

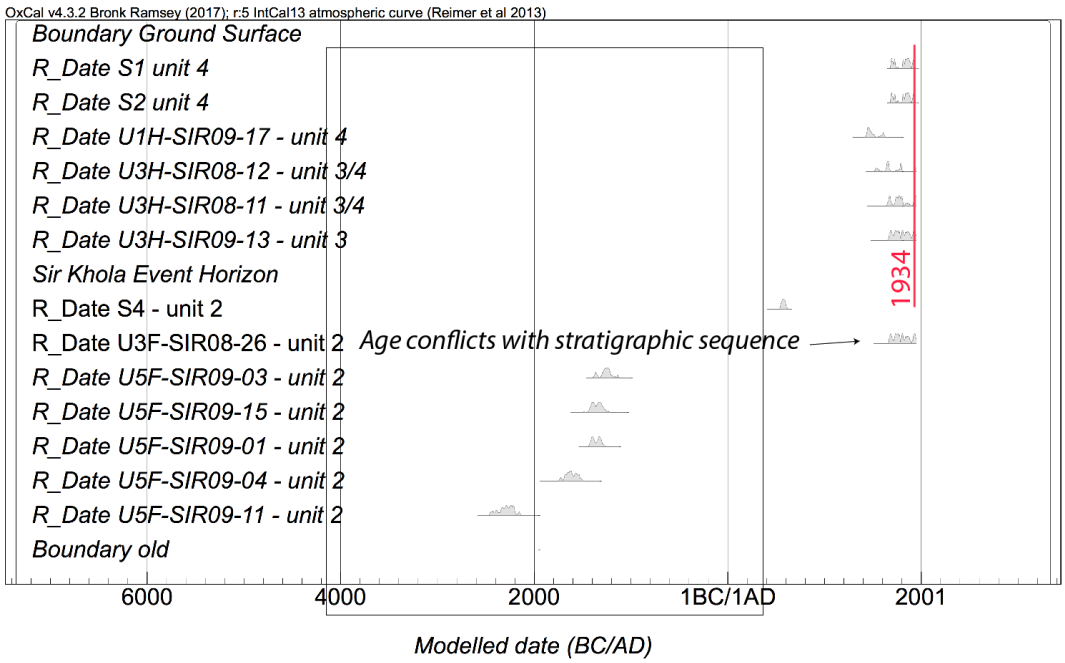

B

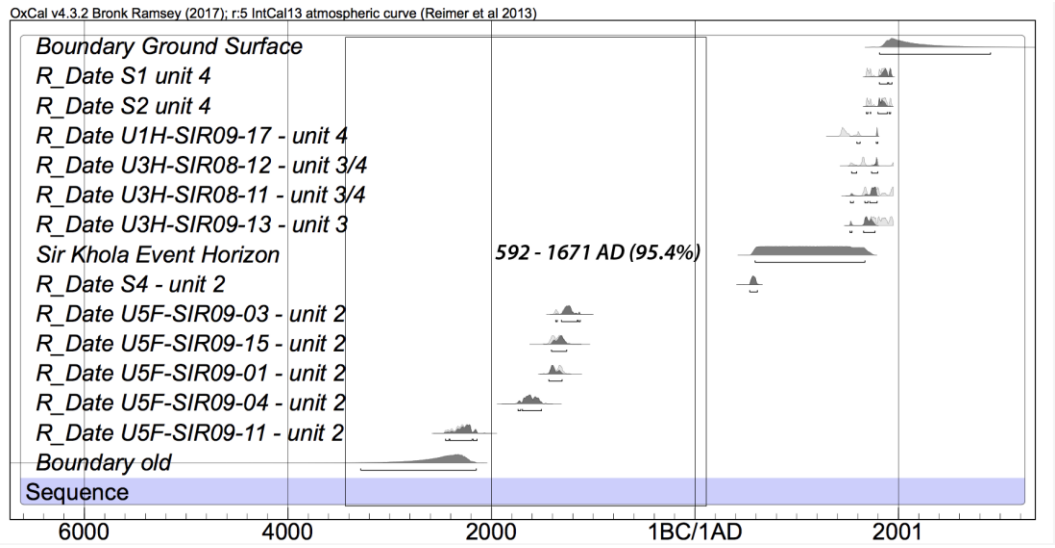

Figure 4c. Plots of corrected radiocarbon ages plotted as function of stratigraphic sequence. A. Unmodeled ages show sample SIR08-26 does not follow stratigraphic sequence and that probability distribution of samples collected above event horizon largely fall well before 1934. B. The event horizon is formally placed by OxCal at between 592-1671 AD when Sir08-26 is not considered in analysis. The analysis is performed with Oxcal v4. 3.2. (https://c14.arch.ox.ac.uk/oxcal/OxCal.html) using the IntCal13 atmospheric curve of Reimer et al. (2013).

References cited in Supplement.

Bollinger, L., Sapkota, S.N., Tapponnier, P., Klinger, Y., Rizza, M., Van der Woerd, J., Tiwari, D.R., Pandey, R., Bitri, A., de Berc, S.B., 2014. Estimating the return times of great Himalayan earthquakes in eastern Nepal: Evidence from the Patu and Bardibas strands of the Main Frontal Thrust. Journal of Geophysical Research-Solid Earth 119, 7123-7163.

Bronk, R., 2009. Bayesian analysis of radicarbon dates. Radiocarbon 51, 337-360.

Reimer, P.J., Bard, E., Bayliss, A., Beck, J.W., Blackwell, P.G., Ramsey, C.B., Buck, C.E., Cheng, H., Edwards, R.L., Friedrich, M., Grootes, P.M., Guilderson, T.P., Haflidason, H., Hajdas, I., Hatte, C., Heaton, T.J., Hoffmann, D.L., Hogg, A.G., Hughen, K.A., Kaiser, K.F., Kromer, B., Manning, S.W., Niu, M., Reimer, R.W., Richards, D.A., Scott, E.M., Southon, J.R., Staff, R.A., Turney, C.S.M., van der Plicht, J., 2013. INTCAL13 and marine13 radiocarbon age calibration curves 0-50,000 years Cal Bp. Radiocarbon 55, 1869-1887.

Sapkota, S.N., Bollinger, L., Klinger, Y., Tapponnier, P., Gaudemer, Y., Tiwari, D., 2013. Primary surface ruptures of the great Himalayan earthquakes in 1934 and 1255. Nature Geoscience 6, 71-76.